Available online at www.sciencedirect.com
ScienceDirect
Journal of Power Sources 172 (2007) 578–586
JOURNAL OF POWER SOURCES
www.elsevier.com/locate/jpowsour

Cryo- and xerogel carbon supported PtRu for DMFC anodes

Catia Arbizzani, Sabina Beninati, Elisa Manferrari, Francesca Soavi, Marina Mastragostino *

Dipartimento di Scienza dei Metalli, Elettrochimica e Tecniche Chimiche, Via San Donato 15, 40127 Bologna, Italy

Received 20 October 2006; received in revised form 11 May 2007; accepted 15 May 2007
Available online 18 May 2007

Abstract

The specific catalytic activity of DMFC anodes based on PtRu may be improved using conducting carbon supports of high surface area and mesoporosity with pore size >20 nm for a high accessible surface area. To this purpose we pursued the strategy of developing PtRu catalysts deposited by chemical and electrochemical route on mesoporous cryo- and xerogel carbons. Here, we report the preparation and characterization data of different mesoporous cryo- and xerogel carbons as well as we present and discuss the results of the structural and morphological study and the catalytic activity data of PtRu catalysts chemically and electrochemically prepared, also by pulse techniques, on such carbons. The results are also compared to those obtained with PtRu supported on the generally used Vulcan carbon support.

Keywords: Cryogel carbon; Xerogel carbon; Carbon supported PtRu; Direct methanol fuel cell catalyst

1. Introduction

Polymer membrane electrolyte fuel cells (PEMFCs) are high efficiency energy conversion systems of great importance in the development of a new sustainable energy economy [1]. Their mid-low operating temperatures require high efficiency electrocatalysts, which consist of Pt and precious metals supported on high surface area carbons, typically on Vulcan XC72 carbon, and the high cost of such electrocatalysts still remains one of the main drawbacks to the wide use of PEMFCs. Direct methanol fuel cells (DMFCs) which are directly fed with liquid fuel, easy to be stored and transported, and that could also take advantage from already existing fuel distribution infrastructures, are particularly attracting and are under study for many applications ranging from portable power sources, to domestic and automotive applications. The target for large-scale automotive application of a low Pt content <0.2 g kW^{-1} at cell voltage of 0.65 V and 80 °C [2], quite stringent for H_2-PEMFCs, is significantly difficult to be reached for DMFCs in which the anode kinetic related to methanol oxidation is greatly slower than that of hydrogen oxidation, and thus requires higher amounts of noble metal. The catalyst of choice for DMFC anode is carbon supported PtRu; in such catalysts the role of Ru is to provide oxygenated species for oxidative removal of CO adsorbed on Pt, as described by the following bifunctional mechanism of methanol electrooxidation:

$$Pt + CH_3OH_{(aq)} \rightarrow Pt\text{–}CH_3OH_{(ads)} \rightarrow Pt\text{–}CO_{(ads)} + 4H^+ + 4e^- \quad (1)$$

$$Ru + H_2O \rightarrow Ru\text{–}OH_{(ads)} + H^+ + e^- \quad (2)$$

$$Pt\text{–}CO_{(ads)} + Ru\text{–}OH_{(ads)} \rightarrow Pt + Ru + CO_2 + H^+ + e^- \quad (3)$$

Much research is focusing on the development of high catalytic activity electrodes for methanol oxidation at low Pt content <1.0 mg cm^{-2}. Basically, two routes are pursued: (i) the development of new catalyst syntheses with attention to alloy composition, nanometric dimensions and uniform distribution of the catalyst on the carbon support and (ii) the development of new carbon supports of high electric conductivity, high surface area and high mesoporosity in the pore size range of 20–40 nm for a high accessible surface area. Indeed, the Nafion binder solution, which is generally used in electrode preparation, is constituted by ionomers that may occlude pores narrower than 20 nm, so that catalyst particles chemically deposited in such pores are not in contact with the proton conductor and the fuel. Even for catalysts electrodeposited on carbon-Nafion support the pore occlusion reduces the carbon surface available for the catalyst and is detrimental for metal dispersion [3–10]. As recently

* Corresponding author. Tel.: +39 051 2099798; fax: +39 051 2099365.
E-mail address: marina.mastragostino@unibo.it (M. Mastragostino).

0378-7753/$ – see front matter © 2007 Elsevier B.V. All rights reserved.
doi:10.1016/j.jpowsour.2007.05.041

reviewed by Liu et al. the catalyst preparation procedures include the impregnation, the colloidal and the microemulsion methods, whereas, the carbon supporting strategies include high surface area carbon blacks, carbon nanotubes and mesoporous carbons such as those obtained by template methods [4]. As it concerns the PtRu synthesis, the impregnation method that consists in the impregnation of the carbon with the PtRu precursors followed by chemical reduction is an easy technique, particularly when $NaBH_4$ is adopted as reducing agent, and yields small PtRu particles which are mainly of 3 nm [5]. Also direct electrodeposition on carbon-Nafion substrate is attracting much attention for its simplicity and versatility, along with the advantage of localizing the catalyst selectively on the surface which will be in direct contact with the fuel, thus providing a high Pt utilization [9–13].

For what regards the carbon supports, cryo- and xerogel carbons are attracting much attention for their high electrical conductivity, high surface area and mesoporosity with narrow pore size distribution, which are tunable by synthesis condition selection. Their preparation, which consists in sol–gel polycondensation of resorcinol with formaldehyde followed by freeze or room temperature (RT) drying and pyrolysis, avoids the supercritical drying step required for the synthesis of aerogel carbons and offers great advantage in terms of cost and safety [14–20].

We already demonstrated that cryogel carbons are promising supports for PtRu catalysts prepared by electrodeposition [21], however, such deposition procedure yielded 50–250 nm PtRu clusters which were too wide to take advantage from the cryogel carbon surface area mainly arising from pores with 20 nm diameter. Furthermore, we inferred that the hydrophobic character typical for cryogel carbon pyrolized at 1050 °C in inert atmosphere, hindering the PtRu aqueous precursor uptake, could be the cause of an uneven dispersion of the catalyst on the carbon support. It has been demonstrated that thermal treatment of carbon in air at $T < 500$ °C induces acid oxygen functional groups (carboxyl, hydroxyl, . . .) on the carbon surface which improve its hydrophilic character [22,23].

Thus, to enhance the metal dispersion on the support and to increase the specific catalytic activity of PtRu for methanol oxidation we have pursued the strategy of developing catalysts based on PtRu chemically prepared *via* the $NaBH_4$ method and electrochemically deposited also by pulse techniques on mesoporous cryo- and xerogel carbons with pores wider than 20 nm, also treated at 400 °C in air before PtRu deposition. The preparation and characterization of different cryo and xerogel carbons and the structure, morphology and catalytic activity of PtRu chemically and electrochemically deposited on such carbons are here reported and discussed to highlight the effect of the carbon support on the electrocatalytic oxidation of methanol.

2. Experimental

2.1. Cryo/xerogel carbon synthesis and characterization

The cryogel carbon C5.7-500 and C7.5-1500 and the xerogel carbons X7.5-1500 and X16-25 were prepared by polycondensation of resorcinol (R, Riedel de Haen, 99.0–100.5%) and formaldehyde (F, 37% aqueous solution, Aldrich) in ultrapure water (W, Milli-Q simplicity system, Millipore Co.) with Na_2CO_3 (C, Riedel de Haen, >99.8%) as gelation catalyst, followed by water/*t*-butanol (Fluka, >99.7%) or water/acetone solvent exchange, freeze (for the cryogel carbons) or RT (for the xerogel carbons) drying and pyrolysis. The resorcinol to formaldehyde molar ratio (R/F) was 0.5 and the dilution factor, i.e. the water to gel precursors molar ratio $D = W/(R + F + C)$, and the resorcinol to gelation catalyst molar ratio (R/C) were 5.7 and 500, 7.5 and 1500, and 16 and 25 for the C5.7-500, C7.5-1500 and X7.5-1500, and X16-25 carbons, respectively, as reported in Table 1. The initial pH value was 6.4 and gelation was performed at 85 °C in sealed vessels for at least 3 days. The freeze-drying was performed at −30, −20 and −10 °C, each temperature being held for 24 h under dynamic vacuum, the RT drying was carried out at ambient pressure for at least 3 days. The pyrolysis step, carried out in a tube furnace (Carbolite) at 1050 °C (2 h, heating rate 10 K min^{-1}, under moderate flux of Argon, 200 cm^3 min^{-1}), was followed by ball milling (20 min at 250 rpm in tungsten jar, Pulverisette Fritsch). Activation of the carbons was performed by thermal treatment in air at 400 °C for 30 min in furnace (ZE Muffle Furnace).

Table 1
Dilution factor ($D = W/(R + C + F)$) and R/C molar ratio used for the synthesis of the cryo- and xerogel carbons and specific total pore volume (V_{tot}), total surface area (S_{BET}) and meso-macropore volume and area of the cryo- and xerogel carbons before and after the activation step and of Vulcan carbon.

Carbons	Synthesis parameters			Porosity			
	D	*R/C*		V_{tot}	S_{BET}	Meso-macropores	
				$cm^3\ g^{-1}$	$m^2\ g^{-1}$	$cm^3\ g^{-1}$	$m^2\ g^{-1}$
C5.7-500 cryogel	5.7	500	Pristine	1.49	605	1.35	285
			Activated	1.94	880	1.72	355
C7.5-1500 cryogel	7.5	1500	Pristine	0.86	570	0.68	110
			Activated	0.99	630	0.76	120
X7.5-1500 xerogel	7.5	1500	Pristine	0.70	420	0.57	110
			Activated	0.97	640	0.76	130
X16-25 xerogel	16	25	Pristine	1.42	585	1.26	205
			Activated	1.56	760	1.34	250
VULCAN	–	–	Pristine	0.51	220	0.45	105

Nitrogen adsorption porosimetry measurements were carried out at 77 K with an ASAP 2020 system (Micromeritics), the carbon powders were dried for at least 2 h at 120 °C, before testing. The total pore volume of the carbons (V_{tot}) was evaluated from the volume of gas adsorbed at the relative pressure $p/p^\circ = 0.99$. The analysis of the N_2 adsorption isotherms by the B.E.T. and B.J.H. theories gave the total specific surface area (S_{BET}) and the mesopore size distribution in the mesopore region in terms of specific volume and surface areas.

2.2. PtRu chemical and electrochemical deposition on carbon supports

Chemical deposition (CD) of PtRu on carbon with a Pt to C mass ratio in the range 5–20% was carried out modifying the method described in ref. [5]; 250 mg of carbon were sonicated for 2 h in 10 mL of H_2PtCl_6–$RuCl_3$ aqueous solution, then 10 mL of $NaBH_4$ aqueous solution in excess with respect to the stoichiometric amount were added and the solution was stirred for 4 h. The solution was filtered and the PtRu/carbon powder was washed with deionized water and dried under vacuum at 80 °C over night.

Electrochemical deposition of PtRu was performed on carbon-Nafion electrodes (ca. 0.8 cm^2) from equimolar aqueous solution 20 mM of H_2PtCl_6 (Fluka, 38% Pt) and $RuCl_3$ (Aldrich, 99.98%) by potentiostatic (ED) and pulsed galvanostatic (GD) or potentiostatic (PD) procedures. The ED electrodeposition consisted in the polarization of the electrodes for 5 s at −58 mV versus NHE followed by 30 s at 742 mV versus NHE, the GD consisted in pulses at $i_{GD} = -25\ mA\ cm^{-2}$ or $-100\ mA\ cm^{-2}$ applied for 5 ms (t_{on}) every 70 ms (t_{off}), and the PD in pulses at −58 mV versus NHE applied with $t_{on} = 50$ ms and $t_{off} = 300$ ms; the ED, GD and PD steps were repeated several times up to 100–200 $\mu g\ cm^{-2}$ of Pt.

The Pt to C mass ratio Pt/C% in the PtRu/carbon powders and PtRu/carbon-Nafion electrodes is given on the basis of the Pt loading checked after powder and electrode mineralization by the tin (II) chloride colorimetric method [24] and of the Pt to Ru atomic ratio as estimated by X-ray diffraction (XRD) analysis.

2.3. PtRu/carbon characterization

XRD measurements were performed with a Philips X'Pert diffractometer, a Cu Kα (λ = 1.5406 Å) radiation source and Ni filter by continuous mode (0.1° 2θ step; $5 \times 10^{-2\circ}$ 2θ s^{-1} scan rate). The crystallite size (d) has been evaluated as average of the values obtained by the Scherrer's equation from the width of the (1 1 1) and (2 2 0) reflexes. The PtRu crystallite atomic composition was evaluated from the trend of the lattice parameter versus Ru content in the alloy reported in Ref. [25].

Scanning electron microscopy observations (SEM) and energy dispersion spectroscopy (EDS) were carried with a ZEISS EVO 50 apparatus equipped with an energy dispersive X-ray analyser from Oxford model INCA ENERGY 350 system.

Transmission electron microscopy (TEM) was performed with a Philips CM 100 apparatus.

The electrodes featured a carbon support loading of 1 mg cm^{-2} and 100–200 $\mu g\ cm^{-2}$ of Pt and, in the case of the tests in conventional electrochemical cells, they were prepared using stainless steel grid current collectors (AISI316L, Delker) coated by spray with carbon (SuperP ERACHEM)–Teflon (60% solution, Dupont) 5:1 wt.% ink in order to reduce contact resistance. The PtRu/carbon catalyst chemically prepared (or the bare carbons in the case of the electrochemically prepared catalyst) was spread on the current collector from ink with 2:1 or 4:1 wt.% carbon-Nafion ultrasonically dispersed in isopropylic alcohol (Merck, >99.7%).

The electrocatalytic activity of the PtRu/carbon-Nafion electrodes was evaluated in 0.1 M H_2SO_4–0.5 M CH_3OH at 60 °C by linear sweep voltammetry (LSV) at 5 mV s^{-1} and chronoamperometry (CA, stirred solution) at different electrode potentials with a polarization time of 600 s. The reported data are averaged over at least four independent measurements for each catalyst system.

CO-stripping tests were performed by flowing CO at ca. 50 $cm^3\ min^{-1}$ for 20 min followed by 20 min Ar bubbling in 0.1 M H_2SO_4 and holding the electrode potential at 260 mV versus NHE; then, the potential was scanned at different rates (0.5–50 mV s^{-1}) from −140 to 860 mV versus NHE. For the CO-stripping measurements glassy carbon electrodes coated by PtRu/carbon-Nafion aqueous inks were used.

All the electrochemical measurements were carried out with a potentiostat/galvanostat Voltalab Radiometer Copenaghen PGZ 301 under argon atmosphere in a cell with separate compartments for the Pt counterelectrode and an Ag/AgCl/HCl 0.04 M or $Hg/Hg_2SO_4/H_2SO_4$ 0.1 M reference electrode; the electrode potentials are expressed in reference to a normal hydrogen electrode (NHE).

2.4. Passive DMFC

The passive DMFCs were assembled with carbon paper backing layers (Hydro2Power) for the anode and cathode coated by spray with catalyst-Nafion-isopropylic alcohol inks. For the anode the PtRu/C5.7-500 (21.1% Pt/C%, C:Nafion 4:1) and PtRu/Vulcan (21.0% Pt/C%, C:Nafion 4:1) catalysts were used, for the cathode the catalyst was Pt chemically deposited on Vulcan (42% Pt/C%, C:Nafion 4:1). A Nafion 115 (Hydro2Power) membrane was treated with H_2O_2 and H_2SO_4 and sandwiched between the two electrodes by hot pressing.

3. Results and discussion

3.1. Carbon support characterization

Table 1 reports the results of the porosity measurements of the cryo- and xerogel carbon powders before and after activation in terms of total and meso-macro specific pore volume and surface area; the data of the Vulcan carbon, which is widely used to support commercial catalyst, are also reported for a comparison. As an example, Fig. 1 shows the N_2 adsorption isotherms of the C5.7-500, X7.5-1500 and X16-25 activated carbons and of the Vulcan carbon, whereas, Fig. 2 shows the corresponding BJH

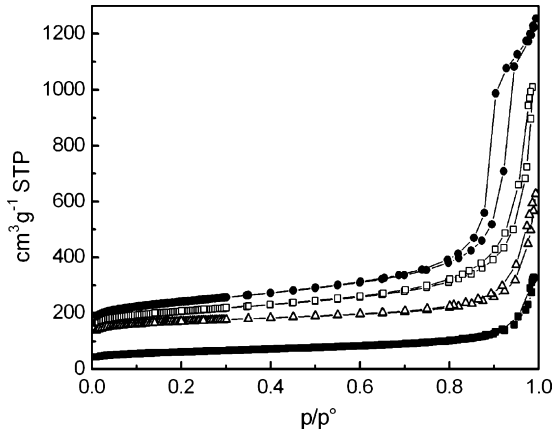

Fig. 1. N_2 adsorption–desorption isotherms at 77 K of the (●) C5.7-500, (△) X7.5-1500, (□) X16-25 activated carbons and of (■) Vulcan carbon.

specific cumulative surface area in the meso-macropore region from the widest to the smallest pores versus pore diameter. Data in Table 1 and Figs. 1 and 2 evidence that different gelation bath compositions (reported in terms gel dilution D and R/C molar ratio) provide cryo- and xerogel carbons with different porosity and significantly higher specific total volume and surface area and, more importantly, higher mesoporosity than that of Vulcan. The carbon featuring the highest mesoporosity is the C5.7-500 cryogel which exhibits 1.35 $cm^3\ g^{-1}$ and 285 $m^2\ g^{-1}$ meso-macropore specific volume and surface area, respectively, and such values increase by 20% after activation. Indeed, the activation step increased the pore volume of all the carbons without modifying their pore size distribution, which ranged from 20 nm (C5.7-500) up to 90 nm (X16-25) with the broader pore size distribution for the higher dilution of the gel precursors. Given that the hardness of the cryogel carbons decreases with the increase of the dilution factor D [14,15], it cannot be excluded that the ball-milling step has affected the pore size distribution, particularly for the xerogel carbon X16-25. The higher values of V_{tot} and S_{BET} of the C7.5-1500 cryogel carbon with respect to those of the X7.5-1500 xerogel prepared with the same

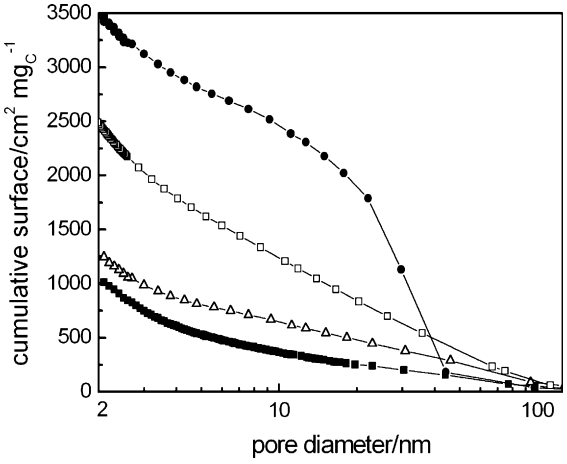

Fig. 2. BJH specific cumulative pore area vs. meso-macropore diameter of the (●) C5.7-500, (△) X7.5-1500, (□) X16-25 activated carbons and of (■) Vulcan carbon.

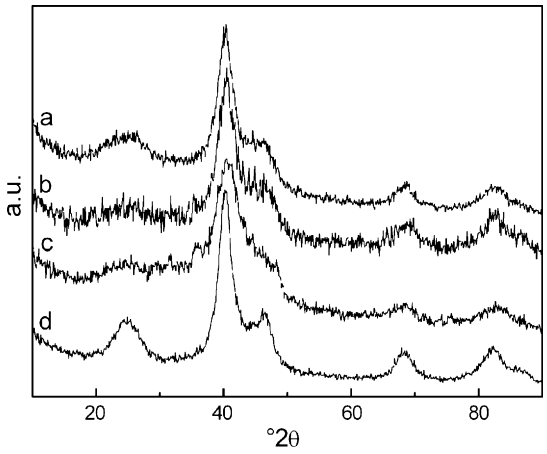

Fig. 3. XRD spectra of PtRu chemically deposited with Pt/C% ca. 10% on the activated carbons (a) C5.7-500, (b) X7.5-1500 and on the pristine carbons, (c) X16-25 pristine and (d) Vulcan.

gelation bath composition indicate that freeze-drying ensures a higher retention of the gel structure upon solvent evaporation with respect to RT drying [15].

3.2. PtRu/carbon chemically prepared

Fig. 3 displays the XRD spectra of PtRu chemically deposited on the activated carbons C5.7-500 and X7.5-1500 and on the pristine X16-25 and Vulcan with a Pt to carbon mass ratio of ca. 10% and Table 2 reports the crystallite size (d) and atomic composition (Pt:Ru) of the different catalysts with Pt/C% ranging from 5 to 20%. The XRD spectra in Fig. 3 and the related data in Table 2 evidence that the crystalline phase of the different catalysts (including that with Vulcan carbon) with Pt/C% ca 10% is quite similar and consists in PtRu alloy with small crystallite size of 2–3 nm and with a slightly excess of Pt with respect to Ru. While in the case of the catalysts supported on the X7.5-1500 and X16-25 carbons the crystallite size and composition does not significantly vary with the increase of the Pt to carbon ratio up to 24.3%, in the case of PtRu chemically deposited on

Table 2
Pt to carbon mass ratio (Pt/C%), crystallite size (d) and atomic composition (Pt:Ru) evaluated by XRD analyses of PtRu chemically (CD) and electrochemically (ED) deposited on the different carbons

PtRu synthesis	Carbon support	Pt/C%	d (nm)	Pt:Ru
CD	C5.7-500	5.4	4.9	70:30
		11.7	2.9	60:40
		21.1	2.6	53:47
	X7.5-1500	4.7	2.8	51:49
		12.2	2.7	54:46
	X16-25[a]	9.8	2.2	51:49
	X16-25	24.3	2.3	52:48
	VULCAN[a]	13.9	2.9	60:40
		21.0	3.8	65:35
ED	C5.7-500[a]	10.7	6.0	85:15

[a] Pristine carbon.

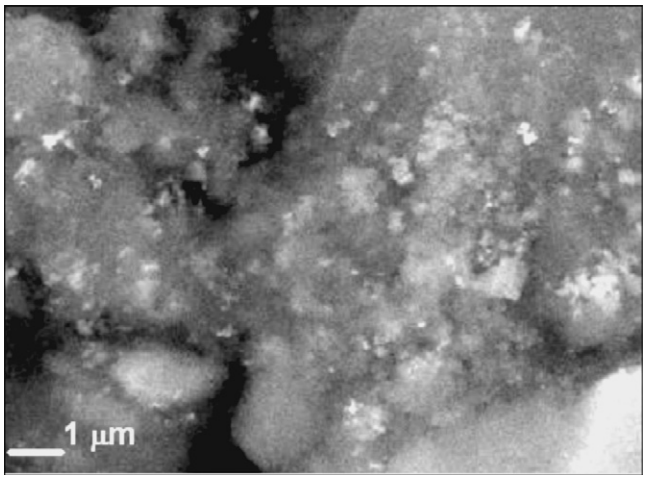

Fig. 4. Backscattered SEM image of PtRu chemically deposited on activated X7.5-1500 xerogel carbon with 12.2% Pt/C%.

the C5.7-500 the crystallite size decreases with the increase of the Pt loading on the support. This is an unexpected result if we consider that the highest catalyst dispersion and the smallest metal particles should be obtained at the lowest Pt/C% ratio. On the other hand, in the PtRu/C5.7-500 catalysts, when the Pt/C% value increases from 5.4 to 21.1%, the Pt:Ru atomic ratio varies from 70:30 to 53:47 and it has been reported that in PtRu alloys the crystallite size decreases with the increase of the Ru content in the alloy [3]. Thus, the data in Table 2 suggest that the main term affecting the crystallite size, which in turn affect the catalytic surface, is the Ru content in the alloy, rather than the carbon support surface area, as also indicated by the comparison of XRD data of PtRu supported on the cryo/xerogel carbons and PtRu/Vulcan. However, EDS measurements revealed a Ru excess in the catalyst layers (Pt:Ru 35:65 for 10% Pt/C%), thus suggesting that amorphous Ru species presumably in the form of oxides are also present. Figs. 4 and 5 which report the backscattered SEM image of PtRu/X7.5-1500 with 12.2% Pt/C% and the results of the TEM analysis of PtRu/C5.7-500 with 21.1% Pt/C%, respectively, evidence that the PtRu crystallites aggregate in nanometric clusters.

The structural and morphological properties of the PtRu deposit seemed not to be affected by the thermal treatment in air of the carbon support. Such activation step enhanced the hydrophilic character of the carbon and the Pt uptake from the precursor aqueous solution by 30%, as well as it improved the PtRu chemical deposition efficiency without affecting the catalytic response as suggested by the results of the activity tests. Table 3 displays the methanol oxidation specific currents (in mA mg^{-1} of Pt) evaluated in 0.1 M H_2SO_4–0.5 M CH_3OH at 60 °C after 600 s at 492 mV versus NHE for electrodes with PtRu chemically deposited with Pt/C% ≥ 5% and C:Nafion weight ratio 4:1 or 2:1; the scattering of the specific current data and Pt loadings for the different samples are also reported. As an example, Fig. 6 reports the methanol oxidation currents at 60 °C of a PtRu/X16-25 electrode chemically prepared with 120 μg of Pt cm^{-2} and 9.8% Pt/C%. Fig. 6a reports the voltammetric current in mA mg^{-1} of Pt during LSV at 5 mV s^{-1} and Fig. 6b reports the cronoamperometric responses in mA cm^{-2} of electrode geometric surface at 542, 492, 442 and 392 mV versus NHE.

The data in Table 3 evidence that for the catalysts PtRu/C5.7-500 and PtRu/X7.5-1500 when Pt/C% is ca. 5% the increase of the Nafion content from C:Nafion 4:1 to 2:1, i.e. the Pt/Nafion% decrease from 20 to 10%, is detrimental for the methanol oxidation currents and such effect is more evident for the PtRu/X7.5-1500 which features carbon support with the lowest mesoporous surface area, thus suggesting that the Nafion film is a barrier for methanol access to PtRu. However, this phenomenon is not relevant with the increase of the Pt/C% and, thus, for Pt/Nafion% >20%.

For each catalyst the catalytic activity decreases with the increase of Pt/C%, presumably because of PtRu particle aggregation that becomes more important with the increase of Pt loading. Though all the carbons which we examined, Vulcan included, feature a mesoporous specific surface area significantly higher than 500 cm^2 mg^{-1}, which almost corresponds to the area required to support a polycrystalline monolayer of Pt with 20% Pt/C% (ca. 1.10^{15} atoms cm^{-2} [26]), such area seems not to be evenly covered by PtRu even for 10% Pt/C%, as shown by the TEM image reported in Fig. 5. This can be explained by considering that with the increase of the Pt loading the metal particles keep depositing on the deposition germs rather than on the support surface still uncovered by the metals.

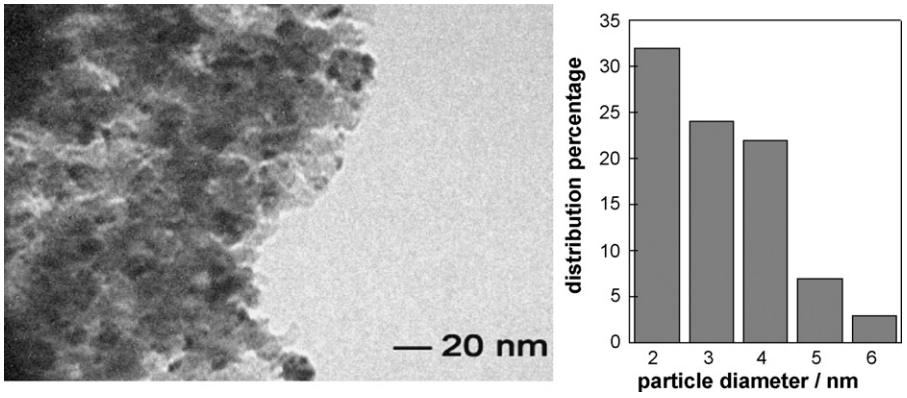

Fig. 5. TEM image and particle size distribution of PtRu chemically deposited on C5.7-500 activated carbon with 21.1% Pt/C%.

Table 3
Specific methanol oxidation current (in mA mg^{-1} of Pt) after 600 s at 492 mV vs. NHE of PtRu chemically (CD) and electrochemically (ED) deposited on different carbon supports with different Pt to carbon and carbon to Nafion mass ratios

PtRu synthesis	Carbon support	Pt/C%	C:Nafion 4:1		C:Nafion 2:1	
			Pt ($\mu g\,cm^{-2}$)	i (mA mg_{Pt}^{-1})	Pt ($\mu g\,cm^{-2}$)	i (mA mg_{Pt}^{-1})
CD	C5.7-500	5.4	64 ± 4	74 ± 19	78 ± 1	60 ± 13
		11.7	100 ± 10	62 ± 9	–	–
		21.1	210 ± 20	46 ± 10	–	–
	X7.5-1500	4.7	52 ± 10	79 ± 20	63 ± 4	38 ± 10
		12.2	90 ± 4	60 ± 9	128 ± 6	56 ± 9
	X16-25[a]	9.8	100 ± 30	63 ± 4	–	–
	X16-25	24.3	205 ± 60	31 ± 4	–	–
	VULCAN[a]	13.9	135 ± 10	34 ± 10	–	–
		21.0	200 ± 50	21 ± 9	–	–
ED	C5.7-500[a]	9 ± 1	–	–	95 ± 13	66 ± 18
	C7.5-1500[a]	10 ± 3	165 ± 45	67 ± 22	135 ± 16	61 ± 17
	C7.5-1500	11 ± 3	–	–	160 ± 55	51 ± 7

[a] Pristine carbon.

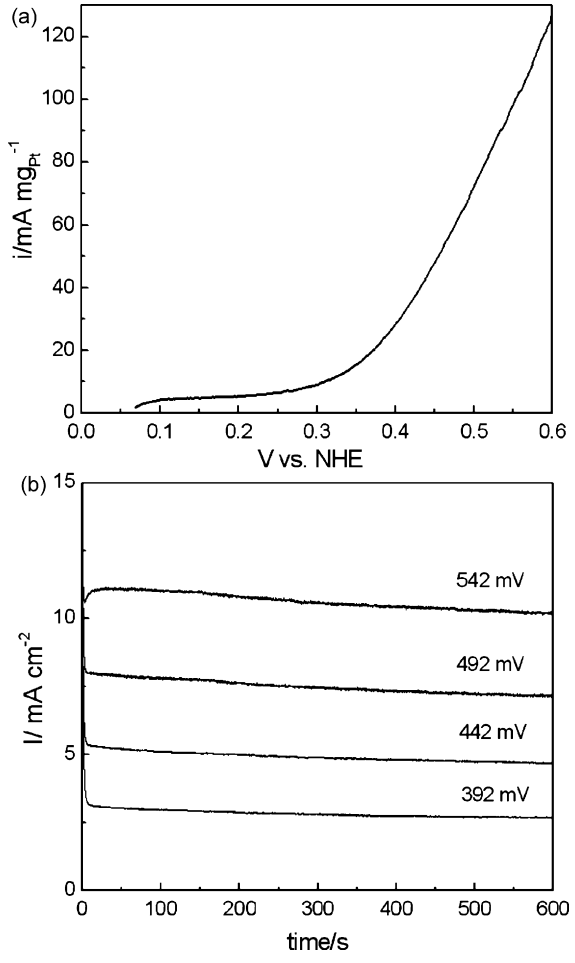

Fig. 6. Methanol oxidation currents (a) in mA mg^{-1} of Pt during LSV at 5 mV s^{-1} and (b) in mA cm^{-2} of electrode geometric surface during CAs recorded at 542, 492, 442 and 392 mV vs. NHE, in 0.1 M H_2SO_4–0.5 M CH_3OH at 60 °C of a PtRu/X16-25 (pristine) electrode chemically prepared with 120 μg of Pt cm^{-2} and a Pt-to-carbon weight ratio of 9.8%.

In Table 3, the catalysts with different cryo/xerogel carbon supports and with the same C:Nafion 4:1 and Pt/C% ≤ 10% ratios perform almost the same; it is not possible to find a clear relation between their catalytic activity, their crystalline features and the porosity of the pristine or activated, cryo/xerogel carbon supports. Only when Pt/C% ≥ 20%, i.e. when PtRu agglomeration may be more important, it is possible to relate the catalytic activity to the carbon support surface area; indeed, for 21–24% Pt/C% the highest catalytic activity (ca. 45 mA mg_{Pt}^{-1}) is reached with the PtRu/C5.7-500 electrodes featuring the carbon support with the highest area developed from the pores >20 nm (ca. 200 $m^2\,g^{-1}$) which provide the best proton and fuel transport in the catalyst layer [6,8].

However, the most evident result in Table 3 is that the catalytic activity of the PtRu catalysts supported on cryo/xerogel carbons are significantly higher (up to double) than those supported on Vulcan. This can be explained by considering that the former carbons have significantly higher surface area from pores wider than 20 nm with respect to the latter, thus provide a higher catalyst surface in contact with fuel. Furthermore, it has to be taken into account that Vulcan, differently from the cryo/xerogel carbons, contains not-negligible amount of sulphur which could bring to Pt poisoning [20].

CO-stripping measurements generally used to evaluate the specific electrochemical active surface area (ECA) of Pt are questionable when applied to PtRu catalysts which can feature alloys of different atomic composition, single metal clusters and metal oxides which can differently contribute to CO oxidation, as also recently reported [27,28]. However, we performed such tests on PtRu/C5.7-500 with 11.7 and 21.1% Pt/C% and on PtRu/Vulcan with 21.0% Pt/C% and the results indicated the following order of ECA: PtRu/C5.7-500 11.7% Pt/C% > PtRu/C5.7-500 21.1% Pt/C% > PtRu/Vulcan 21.0% Pt/C% in agreement with the trend of the catalytic activity reported in Table 3. The ECA values are not reported because the CO-stripping charges were significantly higher than those expected only on the basis of the amount of Pt, even considering it fully active, thus confirming the

important contribute of Ru (inside and outside the PtRu alloy).

Given that the different mesopore size distribution of the investigated carbon supports may affect the distribution of the Nafion binder with different effect on proton conduction in the catalyst layer and, thus, on the catalytic activity, we performed some tests in passive DMFC configuration in which proton conduction is provided only by Nafion. Indeed, the catalytic activities reported in Table 3 may take advantage of the proton conductivity of the H_2SO_4–CH_3OH liquid phase. Two DMFCs (DMFC1 and DMFC2) were assembled with the same cathode (Pt/Vulcan 30%, 1.6 mg cm^{-2} of Pt) and with different anodes; DMFC1 featured PtRu/C5.7-500 (21.1% Pt/C%, 0.17 mg cm^{-2}) and DMFC2 PtRu/Vulcan (21.0% Pt/C%, 0.27 mg cm^{-2}). The anode compartment was filled with 1 M CH_3OH aqueous solution, the cathode was air breathing, and the cells were tested at 60 °C by cronoamperometry at different cell potentials. The specific peak power delivered by DMFC1 after 600 s was 4.7 W g^{-1} of Pt (only the Pt loading in the anode is considered) and the DMFC2's was 2.2 W g^{-1} of Pt; therefore also in passive DMFC configuration the catalytic activity of PtRu/C5.7-500 doubles that of PtRu/Vulcan.

3.3. PtRu/carbon electrochemically prepared

The PtRu was electrochemically deposited on Carbon-Nafion electrodes with C5.7-500 and C7.5-1500 cryogel carbons by ED potentiostatic, and PD and GD pulse potentiostatic and galvanostatic techniques. The ED potentiostatic route provided significantly bigger PtRu alloy crystallites with composition different from that obtained by the CD chemical method. As an example, in Table 2 are reported the XRD data for an ED-PtRu/C5.7-500 electrode which features a *d* value of 6 nm and Pt:Ru ratio of 85:15. Also the morphology of PtRu prepared by ED electrodeposition is very different from that of the chemically prepared, and consists of spherical clusters of 100–250 nm located on the outer surface of the carbon-Nafion electrodes [21], as shown in Fig. 7a by the SEM image of PtRu obtained by ED on C5.7-500-Nafion support. Despite such big clusters the specific catalytic activity of PtRu electrodeposited by ED reported in Table 3 is almost the same than that of the catalysts chemically prepared on the same carbons and is still higher than that of PtRu/Vulcan. Indeed, the fact that in the ED-prepared electrodes the catalyst is located on the outer surface improves the contact with the methanol solution and makes less important the effect of the Nafion distribution in the catalyst layer. Furthermore, the specific methanol oxidation currents reported in Table 3 for ED-PtRu/C7.5-1500 electrodes with pristine and activated carbons are almost the same, thus indicating that also in the case of electrochemically prepared PtRu the activation of the carbon support does not affect the specific catalytic activity.

In order to increase the catalytic surface, thus the specific catalytic activity, we adopted potentiostatic (PD) and galvanostatic (GD) pulse electrodepositions in the ms time scale, which are expected to favour nucleation versus growth of PtRu thus a high dispersion of small particles on the support [12,29–31]. Fig. 7b, c and d are the SEM images of PtRu electrodeposited on C7.5-1500-Nafion by PD (Fig. 7b) and by GD at different current densities (Fig. 7c and d) with almost the same Pt load-

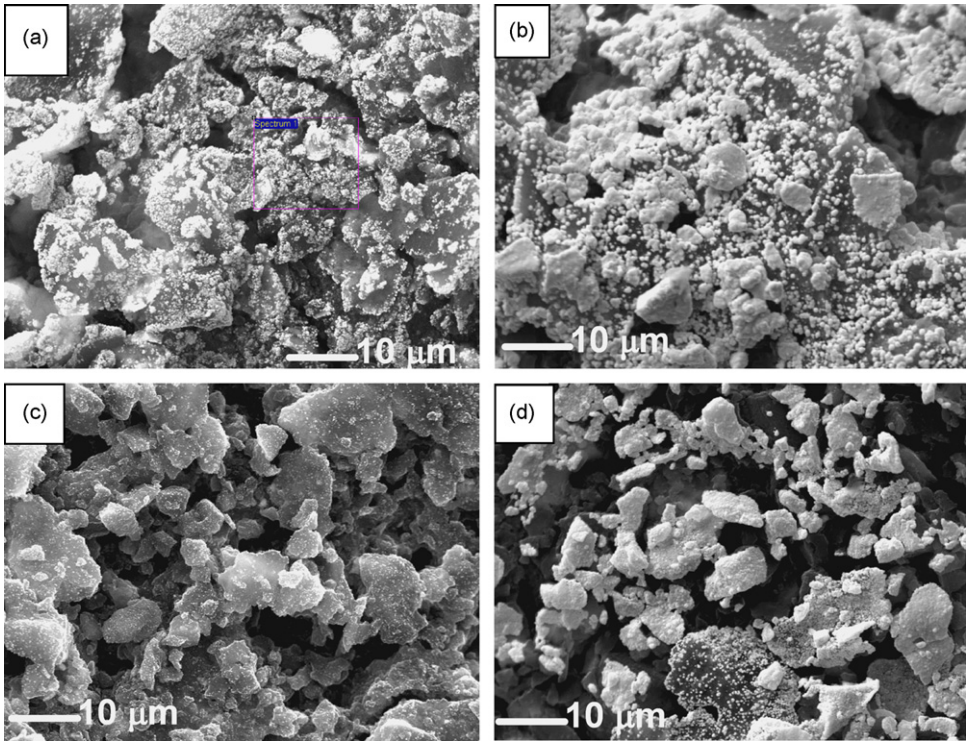

Fig. 7. SEM images of PtRu electrochemically deposited on C5.7-500-Nafion 4:1 by (a) ED (106 µg cm^{-2} of Pt, 9.5% Pt/C%), (b) PD (97 µg cm^{-2} of Pt, 12% Pt/C%), (c) GD at $i_{GD} = -25$ mA cm^{-2} (98 µg cm^{-2} of Pt, 7.8% Pt/C%) and (d) GD at $i_{GD} = -100$ mA cm^{-2} (83 µg cm^{-2} of Pt, 9.3% Pt/C%).

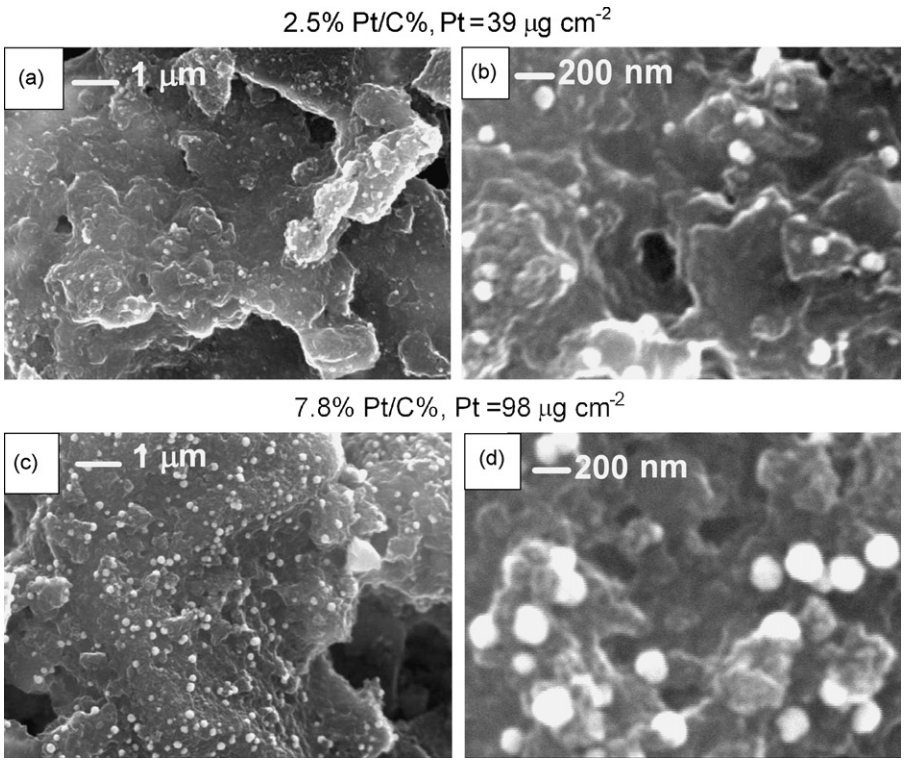

Fig. 8. SEM images at two magnifications of PtRu electrochemically deposited on C5.7-500-Nafion 4:1 by GD at $-25\,mA\,cm^{-2}$ with (a and b) $39\,\mu g\,cm^{-2}$ of Pt and 2.5% Pt/C% and (c and d) $98\,\mu g\,cm^{-2}$ of Pt and 7.8% Pt/C%.

ing of ca. $100\,\mu g\,cm^{-2}$. The different pulsed techniques mainly affected the homogeneity of the catalyst layer distribution on the support rather than the size of the PtRu clusters and the most even dispersion was obtained by GD at $i_{GD} = -25\,mA\,cm^{-2}$ (Fig. 7c), followed by the ED (Fig. 7a) and PD (Fig. 7b) involving deposition currents of $-50/-10\,mA\,cm^{-2}$, and by GD at $i_{GD} = -100\,mA\,cm^{-2}$ (Fig. 7d) that provided the worst distribution with PtRu concentrated only on the most external carbon particles of the electrode. The smallest PtRu particles which we obtained both by potentiostatic and galvanostatic pulses were at least of 50 nm and the main term affecting PtRu particle size seemed to be the Pt loading. This is evidenced by the SEM images reported in Fig. 8 of PtRu/C5.7-500-Nafion electrodes prepared by the same GD at $-25\,mA\,cm^{-2}$ and with different amounts of Pt: when the Pt loading and the Pt/C% are increased from $39\,\mu g\,cm^{-2}$ and 2.5% Pt/C% (Fig. 8a and b) to $98\,\mu g\,cm^{-2}$ and 7.8% Pt/C% (Fig. 8c and d) the PtRu particle size almost doubles. The fact that high electrodeposition current densities concentrate the catalyst only on the most exposed carbon particles to the PtRu precursor solution and that high Pt loadings increase the PtRu cluster size can be explained by considering that after the initial nucleation which takes place mainly on the external surface of the support, PtRu keeps rapidly growing on the more conducting part of the support, i.e. on the PtRu nucleus and this phenomenon is more important with the increase of the deposition rate. Thus, to achieve a homogeneous dispersion of small catalyst particles on the carbon-Nafion support by electrochemical methods low electrodeposition currents and low Pt-to-carbon ratios should be used.

4. Conclusions

The specific catalytic activity of carbon supported PtRu deposited by chemical and electrochemical procedures significantly increases (it is more than double) when Vulcan is substituted by mesoporous cryo- and xerogel carbons also in passive DMFC configuration. The better performance provided by the latter carbon supports with respect to Vulcan may be explained by considering that they feature a high specific surface area from pores wider than 20 nm which may guarantee a better contact among the PtRu, the fuel and the liquid electrolyte or Nafion proton conductor in the case of DMFC assembly. The chemical deposition route provides small PtRu crystallites whose size is not affected by the carbon support mesoporous surface area and with specific catalytic activity that lowers with the increase of the Pt/C% presumably because of agglomeration phenomena. However, we did not find a clear relation between the catalytic activity of the chemically deposited PtRu, its crystalline features and the porosity of the different cryo/xerogel carbon supports. The electrochemical method yields PtRu crystallites with double size with respect to that of the chemically prepared and which grow as spherical clusters on the outer surface of the electrode. Such unsuitable morphology is balanced by the fact that all the electrodeposited catalyst is in direct contact with the methanol solution, so that the specific catalytic activity results almost the same than that of the chemically deposited PtRu. The dispersion of the PtRu clusters on the carbon-Nafion support is affected by the electrodeposition currents, with the most homogeneous catalyst layer obtained at the lowest depo-

sition rates, whereas, the PtRu cluster size increases with the Pt loading, independently from the used electrochemical technique.

The specific catalytic activity of 65 mA mg_{Pt}^{-1} after 600 s at 492 mV versus NHE and 60 °C in 0.1 M H_2SO_4–0.5 M CH_3OH of the cryo- and xerogel carbon supported PtRu is an interesting result which has been obtained with electrodes featuring a Pt/C% of ca. 10% and a low Pt loading of ca. 0.1 mg cm^{-2}, thus sized for portable power source applications which require current densities in the order of 10 mA cm^{-2}. Though further enhancement of the specific catalytic activity of carbon supported PtRu up to the values viable for EV applications, which are in the order of 1.0–0.1 A cm^{-2}, is not feasible by pursuing only the strategy of the optimization of the carbon support morphology, the substitution of Vulcan with cryo/xerogel carbons is a simple and ready-to-be-pursued route that significantly increases the anode catalyst performance.

Acknowledgments

Research funded by MIUR-FISR Italian project "Sviluppo di membrane protoniche composite e di configurazioni elettrodiche innovative per celle a combustibile con elettrolita polimerico".

References

[1] J. Romm, Energy Policy 34 (2006) 2609–2614.
[2] H. Gasteriger, S.S. Kocha, B. Sompalli, F.T. Wagner, Appl. Catal. B 56 (2005) 9–35.
[3] E. Antolini, Mater. Chem. Phys. 78 (2003) 563–573.
[4] H. Liu, C. Song, L. Zhang, J. Zhang, H. Wang, D.P. Wilkinson, J. Power Sources 155 (2006) 95–110.
[5] T.C. Deivaraj, J.Y. Lee, J. Power Sources 142 (2005) 43–49.
[6] M. Uchida, Y. Fukuoka, Y. Sugawara, N. Eda, A. Ohta, J. Electrochem. Soc. 143 (1996) 2245–2252.
[7] V. Raghuveer, A. Manthiram, Electrochem. Solid State Lett. 7 (2004) A336–A339.
[8] V. Rao, P.A. Simonov, E.R. Savinova, G.V. Plaksin, S.V. Cherepanova, G.N. Kryukova, U. Stimming, J. Power Sources 145 (2005) 178–187.
[9] M. Mastragostino, A. Missiroli, F. Soavi, J. Electrochem. Soc. 151 (2004) A1919–A1924.
[10] A. Missiroli, F. Soavi, M. Mastragostino, Electrochem. Solid State Lett. 8 (2005) A110–A114.
[11] H. Kim, B.N. Popov, Electrochem. Solid-State Lett. 7 (2004) A71–A74.
[12] H. Natter, R. Hemplemann, Electrochim. Acta 49 (2003) 51–61.
[13] Z.D. Wei, S.H. Chan, J. Electroanal. Chem. 569 (2004) 23–33.
[14] S.A.A. Muhtaseb, J.A. Ritter, Adv. Mater. 15 (2003) 101–114.
[15] N. Job, A. Théry, R. Pirard, J. Marien, L. Kocon, J.N. Rouzaud, F. Béguin, J.P. Pirard, Carbon 43 (2005) 2481–2494.
[16] H. Tamon, H. Ishizaka, T. Yamamoto, T. Sizuki, Carbon 37 (1999) 2049–2055.
[17] J. Marie, S. Berthon-Fabry, P. Achard, M. Chatenet, A. Pradourat, E. Chainet, J. Non-Cryst. Solids 350 (2004) 88–96.
[18] A. Smirnova, X. Dong, H. Hara, A. Vasiliev, N. Sammes, Int. J. Hydrogen Energy 30 (2005) 149–158.
[19] J.L. Figueiredo, M.F.R. Pereira, P. Serp, P. Kalck, P.V. Samant, J.B. Fernandes, Carbon 44 (2006) 2516–2522.
[20] W.S. Baker, J.W. Long, R.M. Stroud, D.R. Rolison, J. Non-Cryst. Solids 350 (2004) 80–87.
[21] C. Arbizzani, S. Beninati, E. Manferrari, F. Soavi, M. Mastragostino, J. Power Sources 161 (2006) 826–830.
[22] S.W. Hwang, S.H. Hyun, J. Non-Cryst. Solids 247 (2004) 238–245.
[23] S.J. Kim, S.W. Hwang, S.H. Hyun, J. Mater. Sci. 40 (2005) 725–731.
[24] G.H. Ayres, A.S. Meyer, J. Anal. Chem. 23 (1951) 299–304.
[25] M.-S. Löffler, H. Natter, R. Hempelmann, K. Wippermann, Electrochim. Acta 48 (2003) 3047–3051.
[26] J. Fournier, G. Faubert, J.Y. Tilquin, R. Côté, D. Guay, J.P. Dodelet, J. Electrochem. Soc. 144 (1997) 145–154.
[27] H.A. Gasteiger, N. Marković, P.N. Ross, E.J. Cairns, J. Phys. Chem. 98 (1994) 617–625.
[28] T. Vidaković, M. Christov, K. Sundmacher, Electrochim. Acta 52 (2007) 5606–5613.
[29] K.H. Choi, H.S. Kim, T.H. Lee, J. Power Sources 75 (1998) 230–235.
[30] H. Kim, N.P. Subramanian, B.N. Popov, J. Power Sources 138 (2004) 14–24.
[31] Z. He, J. Chen, D. Liu, H. Zhou, Y. Kuang, Diam. Rel. Mater. 13 (2004) 1764–1770.